

Supporting Information

© Wiley-VCH 2010

69451 Weinheim, Germany

Structures of DNA Polymerases Caught Processing Size-Augmented Nucleotide Probes**

*Karin Betz, Frank Streckenbach, Andreas Schnur, Thomas Exner, Wolfram Welte, Kay Diederichs, and Andreas Marx**

anie_200905724_sm_miscellaneous_information.pdf

Supporting Information

Structures of DNA polymerases caught processing size-augmented nucleotide probes

Karin Betz, Frank Streckenbach, Andreas Schnur, Thomas Exner, Wolfram Welte, Kay Diederichs, and Andreas Marx*

Departments of Chemistry and Biology, Konstanz Research School Chemical Biology, Universität Konstanz, Universitätsstrasse 10, 78457 Konstanz (Germany), Fax: (+49)7531-88-5140, andreas.marx@uni-konstanz.de.

Proteins, nucleotides and oligonucleotides

Protein expression and purification were conducted as described.^[1] Modified thymidine-5'-triphosphates dT^RTPs were synthesized as described previously.^[2] Unmodified dNTPs are commercially available (*Roche*).

DNA oligonucleotides for enzyme kinetics were synthesized on an Applied-Biosystems 392 DNA/RNA synthesizer and purified by reversed phase HPLC (DMT-ON) and afterwards by preparative PAGE on a 12% polyacrylamide gel containing 8M urea (DMT-OFF). DNA primer oligonucleotides were labeled with [γ -³²P] ATP using T4 polynucleotide kinase (*Fermentas*) according to the procedure recommended by the manufacturer.

Pre-steady state enzyme kinetics

The rate of single turnover, single nucleotide incorporation was determined using rapid quench flow kinetics on a chemical quench flow apparatus (RQF-3, KinTek Corp., University Park, PA) as previously described.^[3] In brief, 15 μ l of radiolabelled primer/template complex (50 nM) and DNA polymerase (500 nM) in reaction buffer (RQF buffer, Tris*HCl pH 7.5 20mM, NaCl 50mM, MgCl₂ 2mM)^[4] were rapidly mixed with 15 μ l of a dNTP solution in reaction buffer at 37°C. Quenching was achieved by 0.3M EDTA solution (pH 7.0) at defined time intervals. For the investigation of dT^RTP incorporation a 24nt primer (5'-GTG GTG CGA AAT TTC TGA CAG ACA) and a 36nt template (5'-GTG CGT CTG TCA TGT CTG TCA GAA ATT TCG CAC CAC) were applied. Quenched samples were analyzed on a 12% denaturing PAGE followed by phosphor imaging. For kinetic analysis experimental data were fit by nonlinear regression using the program GraphPad Prism 4. The data were fit to a single exponential equation: [conversion]=A*(1-exp(-k_{obs} t)). The observed catalytic rates (k_{obs}) were then plotted against the dNTP concentration used and the data were fitted to a hyperbolic equation [k_{obs}]=k_{cat}*[dNTP]/(K_D + [dNTP]) to determine the K_D and k_{cat} of the incoming nucleotide. The incorporation efficiency is given by k_{pol}/K_D. The depicted data derived from double repeated experiments.

Crystallization and structure determination

The closed ternary complex of the *KlenTaq* bound to DNA primer (5'-d(GAC CAC GGC GC)-3') and template (5'-d(AAA AGG CGC CGT GGT C)-3'), an incorporated ddCMP and the steric probes dT^{Me}TP and dT^{Et}TP crystallized in condition C3 of the commercially available Nucleix Screen from Qiagen (0.2M ammonium acetate, 0.01M magnesium acetate 0.5M sodium cacodylate, pH 6.5 and 30% (w/v) PEG 8000) at 18°C. Purified *KlenTaq* DNA polymerase (14mg/ml), the primer/template complex, ddCTP and the respective steric probe were mixed in a molar ratio of 1:3:10:20 in 20mM Mg₂Cl and crystallized using the vapour diffusion sitting drop method. Datasets from the ternary complexes were collected at the beamline X06SA-PX of the Swiss Light Source (SLS) at the Paul Scherrer

Institut in Villigen, Switzerland, using the wavelength 1.000Å and a PILATUS 6M detector. Data reduction was done with the XDS package^[5] in space group P3₁21 with cell dimensions of a,b=108.7Å, c=90.7Å and a,b=108.8Å, c=90.5Å and to resolutions of 2.2 and 2.0Å for the dT^{Me}TP and dT^{Et}TP trapped structures, respectively. The two structures were solved by difference Fourier techniques. Refinement was performed with PHENIX^[6] and model rebuilding was done with COOT.^[7] Figures of the structures were created in PyMOL.^[8]

Accession numbers

The coordinates and structure factors have been deposited in the Protein Data Bank with the accession numbers 3M8S and 3M8R.

KlenTaq DNA Polymerase mutation, expression, and purification

Mutant I614A was introduced into the *KlenTaq* DNA polymerase ORF via site-directed mutagenesis with the following primers: forward: 5'-d(CCTGGACTATAGCCAGGCAGAGCTCAGGGTGCTG)-3'; reverse: 5'-d(CAGCACCTGAGCTCTGCCTGGCTATAGTCCAGG)-3'. The sequence was determined by DNA sequencing. Expression of the *KlenTaq* DNA polymerases wt and I614A (in pGDR11 vector) was conducted in *E. coli* BL21 (DE3) Gold. Expression cultures were inoculated with 2% of an overnight culture grown at 30°C, and expression was induced at OD₆₀₀ = 0.5 with IPTG at a final concentration of 1 mM. After 4 hr of expression, cultures were centrifuged at 4500xg at 4°C for 10 min. All cultures were grown in LB medium (Roth) with 100 mg/l carbenicillin. Collected cell pellets were resuspended in lysis-buffer (10mM Tris-HCl [pH 9.2], 300mM NaCl, 2.5 mM MgCl₂, 0.1% Triton X-100, 1 mg/ml lysozyme, 5 ml lysis buffer/50 ml culture) and lysed at 37°C for 10 min. *E. coli* proteins were denatured through heating to 75°C for 45 min with a subsequent centrifugation at 15,000xg for 30 min at 4°C. Centrifuged expression lysates were incubated with pre-equilibrated (in 10 mM Tris-HCl [pH 9.2], 0.3 M NaCl, 2.5 mM MgCl₂, 0.1% Triton X-100) NTA-matrix (QIAGEN, 2–3 ml slurry/20 ml lysate) for 60 min at 4°C in an overhead shaker. The NTA matrix was then washed twice with NTA-wash-buffer (10 mM Tris-HCl [pH 9.2], 0.3 M NaCl, 2.5 mM MgCl₂, 0.1% Triton X-100, 20 mM imidazole), and the protein was eluted twice with NTA-elution-buffer (10 mM Tris-HCl [pH 9.2], 0.3 M NaCl, 2.5 mM MgCl₂, 0.1% Triton X-100, 200 mM imidazole). The elution buffer was exchanged by storage buffer (elution buffer without imidazole) using VivaSpins. For storage, glycerol was added to 50%, (NH₄)₂SO₄ to a final concentration of 16 mM and Tween 20 to 0.1%. Enzyme purity was controlled by SDS-PAGE. Protein concentrations were determined using Bradford assay. Purified enzymes were stored at -20°C.

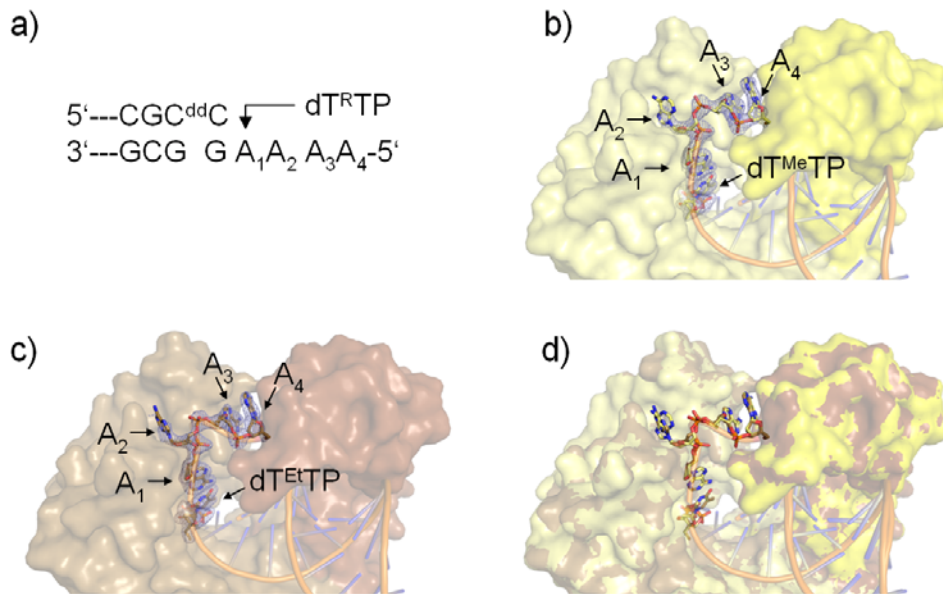


Figure S1. Orientation of single-stranded template strand. a) Numbering template nucleotides. b) Model of structure derived from ternary complex of *KlenTaq*, primer, template, and $\text{dT}^{\text{Me}}\text{TP}$. The respective nucleotides are shown as stick model with carbon atoms in yellow, oxygen atoms in red, nitrogen atoms in blue and phosphorous atoms in orange, and are superimposed with the final refined mFo-DFc simulated annealing omit map. The protein is shown as Connolly surface. c) Same as in b) for complex containing $\text{dT}^{\text{Et}}\text{TP}$. d) Superposition of structures depicted in b) and c) using the same colour code.

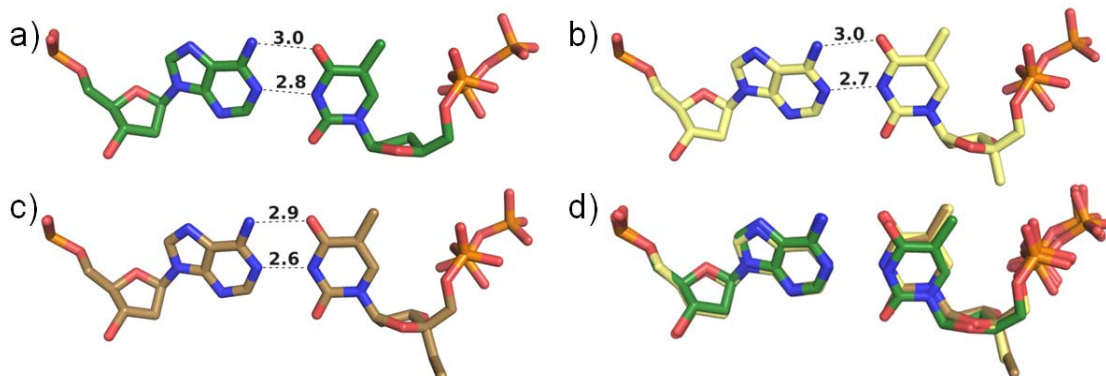


Figure S2. Close-up view on coding adenosine and incoming thymidine analogue. a) Stick model of structure derived from ternary complex of *KlenTaq*, primer, template, and $\text{ddT}^{\text{H}}\text{TP}$ (pdb: 1QTM). The indicated distances were determined by PyMOL and are shown in Å. b) Same as in a) for complex containing $\text{dT}^{\text{Me}}\text{TP}$. c) Same as in a) for complex containing $\text{dT}^{\text{Et}}\text{TP}$. d) Superposition of structures depicted in a)-c) using the colour code of Figure 1.

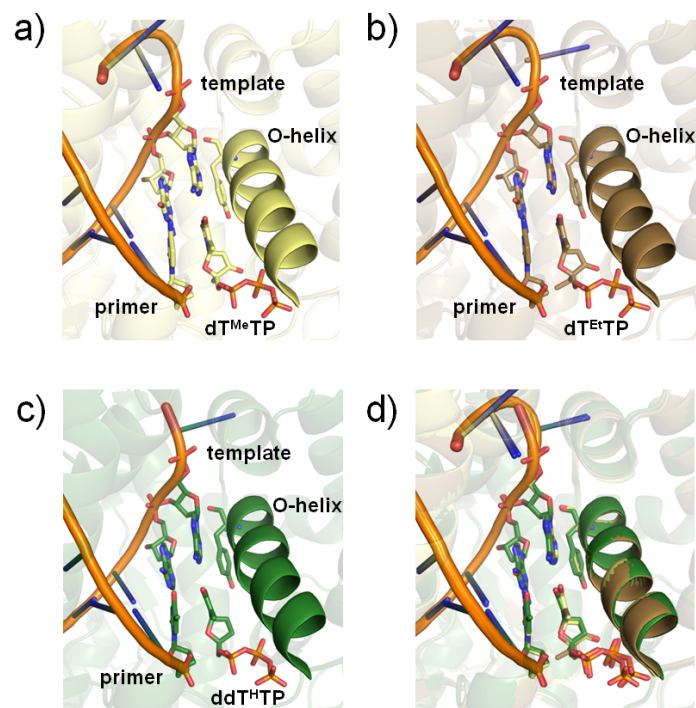


Figure S3. Close-up views highlighting the conformation of the O-helix. a) Ternary complex of *KlenTaq*, primer, template, and dT^{Me}TP. The primer terminus and the nascent nucleotide pair are depicted in sticks. b) Same as in a) for complex containing dT^{Et}TP. c) Same as in a) using the reported data containing ddT^HTP (pdb: 1QTM). d) Superposition of structures depicted in a)-c) using the colour code of Figure 1.

Table S1. Summary of crystallographic data

Crystal	<i>KlenTaq</i> dT ^{Me} -TP	<i>KlenTaq</i> dT ^{Et} -TP
Data collection		
Wavelength (Å)	1.000	1.000
Resolution (Å) ^a	47.1-2.20 (2.33-2.20)	47.1-2.00 (2.12-2.00)
Total reflections ^a	311920 (46718)	420922 (67045)
Unique reflections ^a	46718 (5046)	42216 (6678)
Completeness (%) ^a	99.7 (98.3)	99.8 (98.6)
Mean I/σ ^a	12.9 (1.9)	22.1 (2.6)
R _{meas} (%) ^a	11.5 (105.2)	7.5 (87.9)
Refinement		
Resolution range (Å) ^a	47.1-2.20 (2.27-2.20)	47.1-2.00 (2.05-2.00)
R _{cryst} (%) ^a	17.0 (25.8)	18.0 (21.6)
R _{free} (%) ^a	22.4 (36.2)	22.1 (28.0)
Protein residues	539	539
DNA (primer/template)	12/16	12/16
nucleotides	dT ^{Me} -TP	dT ^{Et} -TP
Water molecules	123	304
Mg ²⁺ ions	2	2
<u>Average B factors (Å²)</u>		
Protein	44.4	47.9
DNA	40.6	39.8
dT ^R -TP	33.4	39.7
<u>r.m.s. deviations</u>		
Bond length (Å)	0.012	0.011
Bond angle (°)	0.97	0.83
Max. likelihood estimate for coord. error (Å)	0.27	0.26
Ramachandran outliers	1	1

R_{meas} = redundancy independent R-factor (intensities)

(For definition of R_{meas} see Diederichs, K. & Karplus, P. A. *Nature Struct. Biol.* **4**, 269-275 (1997))

^aValues in parentheses correspond to those in the outer resolution shell

Table S2. P-values of sugar moieties in primer, template and nucleotides of the structures containing dT^{Me}-TP and dT^{Et}-TP, respectively determined using the PROSIT server.^[9] It should be noted that the P-value (column 7) was not specifically restrained during refinement in phenix.refine.

dT^{Me}-Template												
No.	V ₀	V ₁	V ₂	V ₃	V ₄	P	vmax	χ	γ	TYPE		
A	-13,4	25,0	-26,6	19,4	-3,9	169,5	27,0	-127,9	50,8	C2'-endo	B-Form	Southern
A	-31,8	45,2	-40,7	23,8	4,8	155,2	44,8	99,3	43,2	C2'-endo	B-Form	Southern
A	-6,5	-17,4	33,2	-37,8	28,0	28,2	37,6	4,6	60,3	C3'-endo	A-Form	Northern
A	7,5	-25,1	32,2	-29,0	13,6	5,7	32,4	-171,5	177,9	C3'-endo	A-Form	Northern
G	2,7	-27,6	40,0	-39,6	23,5	14,9	41,4	-160,0	52,8	C3'-endo	A-Form	Northern
G	-4,1	-22,4	38,7	-42,2	29,1	24,0	42,3	-148,7	43,7	C3'-endo	A-Form	Northern
C	-2,2	-17,4	28,9	-30,9	21,1	22,5	31,3	-169,5	177,8	C3'-endo	A-Form	Northern
G	-14,1	29,2	-32,3	25,2	-7,2	173,8	32,5	-105,6	50,3	C2'-endo	B-Form	Southern
C	-14,0	29,0	-32,2	25,0	-7,1	173,8	32,4	-98,7	39,5	C2'-endo	B-Form	Southern
C	-9,1	-9,7	23,5	-29,4	24,3	36,3	29,1	-141,9	45,4	C4'-exo	A-Form	Northern
G	-13,8	25,7	-27,4	20,0	-4,1	169,6	27,8	-110,6	51,1	C2'-endo	B-Form	Southern
T	-29,6	36,6	-29,9	13,6	9,9	145,8	36,1	-110,9	47,5	C1'-exo	B-Form	Southern
G	-34,1	37,7	-27,1	8,3	16,0	136,3	37,4	-106,3	43,8	C1'-exo	B-Form	Southern
G	-37,9	34,4	-18,5	-2,8	25,3	119,5	37,5	-114,2	36,2	C1'-exo	B-Form	Southern
T	-37,8	38,2	-24,5	3,4	21,5	128,7	39,2	-131,2	57,8	C1'-exo	B-Form	Southern
C	-40,4	44,1	-31,3	9,0	19,5	135,4	44,0	-117,0	46,9	C1'-exo	B-Form	Southern
dT^{Me}-Primer												
No.	V ₀	V ₁	V ₂	V ₃	V ₄	P	vmax	χ	γ	TYPE		
G	-14,8	-11,9	32,1	-41,5	35,5	39,0	41,2	-166,7	-10,6	C4'-exo	A-Form	Northern
A	-8,0	-1,6	9,9	-14,8	14,4	49,4	15,3	-137,1	46,0	C4'-exo	A-Form	Northern
C	23,2	-30,3	25,7	-13,1	-6,2	329,5	29,8	-157,0	-144,9	C2'-exo	A-Form	Northern
C	-21,8	10,9	3,1	-15,7	23,7	82,5	23,6	-138,1	38,9	O4'-endo	A-Form	Northern
A	-9,5	28,4	-35,8	31,1	-13,8	183,7	35,8	-102,8	46,7	C3'-exo	B-Form	Southern
C	-34,8	23,0	-3,5	-16,6	32,5	95,8	34,9	-118,7	43,8	O4'-endo	B-Form	Southern
G	-30,8	36,1	-28,0	11,1	12,2	141,7	35,6	-106,3	49,1	C1'-exo	B-Form	Southern
G	-38,7	28,0	-7,4	-14,8	33,6	101,1	38,1	-120,9	44,2	O4'-endo	B-Form	Southern
C	-34,7	44,5	-37,0	18,1	10,2	147,9	43,6	-96,0	50,5	C2'-endo	B-Form	Southern
G	3,1	-27,3	39,4	-38,7	22,8	14,4	40,7	-149,6	38,0	C3'-endo	A-Form	Northern
C	-3,8	-18,7	32,6	-35,8	25,1	24,7	35,9	-151,6	49,2	C3'-endo	A-Form	Northern
ddC	8,5	-21,3	25,3	-21,2	8,1	359,6	25,3	-149,5	73,0	C3'-endo	A-Form	Northern
dT ^{Me} -TP	21,7	-37,2	38,0	-24,7	1,2	344,3	39,5	-138,0	63,4	C2'-exo	A-Form	Northern

dT^{Et}-Template

No.	V ₀	V ₁	V ₂	V ₃	V ₄	P	vmax	χ	γ	TYPE		
A	-19,8	33,0	-33,0	22,5	-1,9	164,4	34,3	-114,9	49,3	C2'-endo	B-Form	Southern
A	-33,6	47,3	-42,4	24,5	5,5	154,6	47,0	90,3	45,5	C2'-endo	B-Form	Southern
A	26,9	-31,6	24,5	-9,6	-10,7	321,7	31,2	171,1	-40,7	C2'-exo	A-Form	Northern
A	4,4	-23,4	32,3	-30,7	16,7	11,1	32,9	-174,6	179,2	C3'-endo	A-Form	Northern
G	0,3	-25,0	38,8	-40,0	25,0	18,4	40,9	-161,2	53,2	C3'-endo	A-Form	Northern
G	-3,1	-22,2	37,3	-40,1	27,3	22,8	40,4	-149,7	45,1	C3'-endo	A-Form	Northern
C	-7,5	-13,7	28,1	-33,2	26,0	31,5	33,0	-173,6	178,5	C3'-endo	A-Form	Northern
G	-14,9	28,8	-30,9	23,3	-5,6	171,2	31,3	-104,9	51,9	C2'-endo	B-Form	Southern
C	-19,6	29,9	-28,3	17,8	1,0	159,4	30,2	-106,9	44,2	C2'-endo	B-Form	Southern
C	-12,4	-5,9	20,5	-28,3	25,7	43,8	28,4	-142,8	42,2	C4'-exo	A-Form	Northern
G	-12,7	23,1	-24,4	17,8	-3,3	168,8	24,9	-107,6	47,8	C2'-endo	B-Form	Southern
T	-33,2	35,1	-24,4	6,0	17,0	133,4	35,5	-118,5	53,6	C1'-exo	B-Form	Southern
G	-34,5	32,1	-18,1	-1,3	22,4	121,7	34,4	-113,4	41,6	C1'-exo	B-Form	Southern
G	-35,5	34,3	-20,4	0,5	21,9	124,6	36,0	-117,9	49,7	C1'-exo	B-Form	Southern
T	-43,8	35,7	-14,9	-10,0	33,6	110,4	42,7	-136,4	58,9	O4'-endo	B-Form	Southern
C	-37,1	46,7	-38,0	17,9	11,8	146,4	45,6	-108,9	46,3	C2'-endo	B-Form	Southern

dT^{Et}-Primer

No.	V ₀	V ₁	V ₂	V ₃	V ₄	P	vmax	χ	γ	TYPE		
G	-11,8	-13,4	31,6	-39,5	32,2	35,8	39,0	-161,0	-15,3	C3'-endo	A-Form	Northern
A	-1,0	-16,6	26,6	-27,9	18,3	20,4	28,4	-148,0	52,8	C3'-endo	A-Form	Northern
C	25,1	-29,9	23,2	-9,4	-9,8	322,2	29,4	-146,5	-103,5	C2'-exo	A-Form	Northern
C	-27,4	27,5	-17,5	2,2	15,7	128,2	28,3	-127,5	46,4	C1'-exo	B-Form	Southern
A	-13,6	29,5	-33,4	26,4	-8,2	175,3	33,5	-104,3	37,3	C2'-endo	B-Form	Southern
C	-37,6	24,5	-3,6	-18,0	35,1	95,4	37,6	-121,9	45,7	O4'-endo	B-Form	Southern
G	-30,8	35,7	-27,1	10,1	12,9	140,3	35,3	-107,3	52,0	C1'-exo	B-Form	Southern
G	-42,6	32,7	-10,9	-13,4	35,0	105,2	41,6	-120,8	41,8	O4'-endo	B-Form	Southern
C	-34,5	45,8	-39,1	20,6	8,5	150,5	44,9	-91,4	46,8	C2'-endo	B-Form	Southern
G	2,0	-27,2	40,2	-40,0	24,4	15,9	41,8	-151,4	37,4	C3'-endo	A-Form	Northern
C	-7,5	-16,5	32,5	-37,8	28,7	29,9	37,5	-149,9	54,2	C3'-endo	A-Form	Northern
ddC	10,4	-25,6	29,4	-25,1	9,3	359,0	29,4	-149,2	56,2	C2'-exo	A-Form	Northern
dT ^{Et} -TP	20,3	-38,2	40,9	-28,2	4,5	348,4	41,7	-139,2	66,3	C2'-exo	A-Form	Northern

Table S3. Motif A consensus sequence alignment

Thermus aquaticus	DYSQ I ELR
Thermus thermophilus	DYSQ I ELR
Thermus caldophilus	DYSQ I ELR
Thermus filiformis	DYSQ I ELR
Rickettsia felis	DYSQ I ELR
Mycobacterium tuberculosis	DYSQ I EMR
Homo sapiens (pol theta)	DYSQ I ELR
Escherichia coli (pol I)	DYSQ I ELR
Chlamydia trachomatis (pol I)	DYSQ I ELR
Chlamydia pneumoniae (pol I)	DYSQ I ELR
Treponema pallidum (pol I)	DYSQ I ELV
Methylobacterium (pol I)	DYSQ I ELR
Deinococcus radiodurans (pol I)	DYSQ I ELR
Helicobacter pylori (pol I)	DYSQ I ELR
Borrelia burgdorferi (pol I)	DYSQ I ELA
Bacillus subtilis (pol I)	DYSQ I ELR

References

- [1] a) Y. Li, Y. Kong, S. Korolev, G. Waksman, *Protein* **1998**, *7*, 1116-23. b) Korolev, M. Nayal, W. M. Barnes, E. Di Cera, G. Waksman, *Proc. Natl. Acad. Sci. USA* **1995**, *92*, 9264-8. c) Y. Li, S. Korolev, G. Waksman, *EMBO J.* **1998**, *17*, 7514-25. d) Y. Li, V. Mitaxov, G. Waksman, *Proc. Natl. Acad. Sci. USA* **1999**, *96*, 9491-6. e) Y. Li, G. Waksman, *Protein Sci.* **2001**, *10*, 1225-33.
- [2] Streckenbach, G. Rangam, H. M. Möller, A. Marx, *ChemBioChem* **2009**, *10*, 1630-1633.
- [3] F. Di Pasquale, D. Fischer, D. Grohmann, T. Restle, A. Geyer, A. Marx, *J. Am. Chem. Soc.* **2008**, *130*, 10748-10757.
- [4] P. J. Rothwell, V. Mitaksov, G. Waksman, *Mol. Cell* **2005**, *19*, 345-355.
- [5] W. Kabsch, *J. Appl. Cryst.* **1993**, *26*, 795-800.
- [6] P. D. Adams, R. W. Grosse-Kunstleve, L.-W. Hung, T. R. Ioerger, A. J. McCoy, N. W. Moriarty, R. J. Read, J. C. Sacchettini, N. K. Sauter, T. C. Terwilliger, *Acta Cryst.* **2002**, *D58*, 1948-1954.
- [7] P. Emsley, K. Cowtan, *Acta Cryst.* **2004**, *D60*, 2126-2132.
- [8] W. L. DeLano, DeLano Scientific, Palo Alto, CA, USA **2002**.
- [9] G. Sun, J.H. Voigt, I.V. Filippov, V.E. Marquez, M.C. Nicklaus, *J Chem Inf Comput Sci*, **2004**, *44*, 1752-1762.